TEMPLATING OF MULTIPLE LIGAND METAL-ION COMPLEXATION SITES IN 8-HYDROXYQUINOLINE-MODIFIED SILICA SOL-GEL MATERIALS INVESTIGATED BY *IN SITU* RAMAN SPECTROSCOPY

Rory H. Uibel and Joel M. Harris*
Department of Chemistry
University of Utah
315 South 1400 East
Salt Lake City, UT 84112-0850

ABSTRACT

Metal-ion templating in a sol-gel synthesis is used to develop multi-ligand 8-hydroxyquinoline binding sites in porous silica structures. The acid-base equilibria and the metal-ion binding equilibria and stoichiometry of these materials are investigated by *in situ* Raman spectroscopy. This technique is capable of resolving spectral responses of the free ligand, its acid-base forms along the monomeric and dimeric ligand complexes with Cu^{2+}. The proton-transfer equilibrium constants and first-ligand binding equilibrium constant to Cu^{2+} for the metal-ion templated silica are equivalent to surface-immobilized 8HQ on silica gel. The second ligand binding constant to Cu^{2+}, however, is comparable to the first ligand binding constant, which differs from free-solution behavior, where an order-of-magnitude smaller value is expected. The free energy available for binding the second ligand within the templated material is comparable to the first ligand, probably due to the nearly optimal location of the second ligand for binding, based on the templating that is done during this synthesis. The metal-ion concentration responses of sol-gels prepared with varying amounts of metal ion during the syntheses were also tested, and the results indicate control over the fraction of templated binding sites.

INTRODUCTION

Chemical modification of high surface-area materials with immobilized ligands is a strategy for solving problems in a variety of areas, including clean up of metals from waste streams, separation of metal-ion species, or preconcentration of metal ions for trace-level detection. Recent progress has been made in synthesis of ligands that can be bound onto high surface-area silica supports [1-6]. One of the most widely used silica-immobilized metal chelating reagents for preconcentration of trace elements is 8-hydroxyquinoline (8HQ) [7-10]. This ligand exhibits a high affinity for a variety of transition metals while rejecting the alkaline-earth species [10]. More than 60 metals can react with 8HQ to form complexes, with formation constants in solution ranging from 10^4 (Ba^{2+}) to 10^{49} (Ga^{3+}) [10,11].

In free-solution complexation by 8HQ, the coordination of metal ions with excess ligand occurs with a stoichiometry that is generally the same as the metal-ion charge [11]. For example, Cu^{2+} forms a binary 8HQ complex in free solution with formation constants 10^{12} and 10^{11} for binding the first and second ligand, respectively [11]. When the ligand is bound to silica or controlled-pore glass surfaces [8,9,12-14], however, the complexation ligand-to-metal ratio for silica-immobilized 8HQ has been reported to be 1:1. One disadvantage of these column elution studies for determining the ligand stoichiometry is that the total binding capacity of the material was measured, without the ability to distinguish between different ligand complexes on the surface. The ligand-to-metal ratio depends on the *local* concentration of ligands on the surface, the surface geometry of the support, and the ligand tether flexibility. With these factors in mind, it could be possible to have a heterogeneous surface that exhibits a variety of local ligand-to-metal ratios.

In recent studies from this lab [15,16], fiber-optic Raman spectroscopy was applied to the *in situ* monitoring of metal-ion complexation to immobilized ligands. This method is capable of distinguishing between various forms of the surface-bound ligand, where the protonated,

neutral, and metal-ion complexed forms of silica-immobilized 8HQ can be resolved. This methodology has been used in a batch-mode experiment to monitor a titration of a known amount of silica-immobilized phenylazo-linked 8HQ with varying amounts of copper ion to determine whether higher order ligand-to-metal complexes could be observed [15]. The spectra, acquired at various added metal-ion/ligand ratios in the sample ranging from 0.1 to 3, could be fit to a linear combination of two components, the spectra of uncomplexed ligand and the single 1:1 complex. When the metal-ion/ligand ratio in the sample was 0.5, the contributions of each of these species were equal, which is also the signature of a 1:1 complex. These results indicate that the phenylazo-linked ligands immobilized on silica are spaced too far apart on the surface and lack sufficient flexibility to form a higher-order complexes with a divalent metal ion.

The inability of surface-immobilized 8HQ to form multiple ligand complexes with higher valency metal ions limits the selectivity and complexation free energy available for preconcentration or the sequestering metal ion activity from solutions at low concentrations. While longer and more flexible tethers for binding ligands to the surface might be employed, the use of larger tethers would likely further reduce the surface coverage so that higher-order complexes would still be relatively rare on the surface. The approach to generating higher-order metal-complexes with immobilized 8HQ that is adopted in this work is to build the silica-framework around a preformed metal-complex using a silica sol-gel synthesis. This templating approach to developing selective metal-ion binding materials was first developed for polymers [17-21] where, for example, acrylic or methacrylic acid [17,18], polyethyleneimine oligomers [19], or organophosphorous monomers [20] are preorganized by complexation with a target metal ion prior to cross-linking of the polymer material. More recently, metal-ion templating has been implemented in sol-gel materials by incorporating silane-bound ethylenediamine ligands into the sol-gel synthesis [22-26] producing mesoporous silica xerogels [22-24], titania thin-films [25],

and hybrid organic-inorganic polymers [26], which serve as selective materials for metal-ion binding.

In the present work, the concept of using metal-ion templating in a sol-gel synthesis is extended to the development of multi-ligand 8-hydroxyquinoline binding sites in silica materials. The stoichiometry of the materials is investigated using *in situ* Raman spectroscopy measurements that are capable of resolving spectra of the free ligand and the monomeric and dimeric ligand complexes with Cu^{2+}. The metal-ion concentration responses of sol-gel materials prepared with and without the templating steps are compared.

EXPERIMENTAL SECTION

Synthesis of immobilized templated ligand. The synthesis of the sol-gel material was carried out by the method first developed by Stöber [27], as modified by van Blaaderen [28], with further modifications described below for the templating of the 8-hydroxyquinoline ligand (see Figure 1). Chemicals used for this synthesis were 8-hydroxyquinoline, sodium nitrite, sodium hydroxide, tetraethoxysilane (Aldrich), methanol, cupric chloride (Mallinckrodt), p-aminophenyltrimethoxysilane (Gelest). All reagents were used as received. Water used for this reaction was deionized, quartz-distilled, and filtered (Nanopure II, Barnstead).

The initial synthesis of the silane-linked ligand is a modification [9,29] of a reaction described by Long and Schofield [30], whereby a diazonium salt of an aromatic amine is coupled to 8-hydroxyquinoline via an azo linkage. The reaction begins with dissolving equal molar amounts of 8-hydroxyquinoline and p-aminophenyltrimethoxysilane (0.04 mmol) into 10 mL of water containing 0.08 mmol HCl in a 100 mL round bottom flask. This mixture was magnetically stirred for 2 h at room temperature to bring both molecules into solution; the final solution exhibits a slight yellow color. After everything had dissolved, the flask was placed in an ice bath to cool for 2 h with continued stirring. Then 0.006 mmol of sodium nitrite was added to

the mixture, and the resulting suspension was stirred and cooled on ice for 12 h. Indication that the reaction was proceeding was apparent from the change in solution color to a light red color after ca. 2h. To allow complexation with the metal ion, the solution pH was adjusted to a value of ~8.0 by adding 0.18 mmol of sodium hydroxide. Next, 0.02 mmol of cupric chloride was added, to produce a ligand/metal ratio of 2/1. The suspension was then stirred for another 20 minutes; longer times could result in cross linking of the trimethoxysilane groups on the ligand. Then 80 mL of methanol and 26 mmol of tetraethoxysilane (650 times excess of the ligand) were added to the mixture and stirred for an additional 12 h. This procedure produces porous sol-gel particles; if the final solution is allowed to react for more than ~16 h, further cross-linking occurs within the pores, and the templated metal ions cannot be removed from the sol-gel material. Upon completion of the reaction, the product was filtered and washed with methanol, and water.

Elemental analysis (MHW Laboratories, Phoenix) of the final product yielded 0.43 ($\pm$ 0.01) % C, and 0.10 ($\pm$ 0.005) % N. Since the blank sol-gel material does not contain detectable carbon or nitrogen, one can use this analysis to estimate the SiO_2 / ligand ratio. For each gram of material, 0.43 % C would result in 24 μmol of ligand per gram of sol-gel material by the following expression: 4.3 mg / (12 g/mol *15) = 24 μmol of ligand, which is consistent with a similar estimate of specific ligand fraction obtained from the % N in the material. To determine the amount of SiO_2 in a 1 g sample, one can subtract the mass of the bound ligand:metal complex with the following expression 1.0 - 0.0043 (C) - 0.001(N) - 0.0005 (Cu and H) = 0.994 g SiO_2. This would result in ~16.8 mmol of SiO_2 which results in a SiO_2 / ligand ratio of ~700. This ratio corresponds, within the analysis uncertainty, to the expected 650-times molar excess of tetraethoxysilane relative to the ligand that was available in the reaction mixture. The elemental analysis results can also be used to verify the extent of the first reaction whereby 8-hydroxyquinoline was linked to the amine silane via the azo linkage (see Figure 1).

The theoretical nitrogen/carbon (N/C) ratio of the azo-linked product is 0.233; if the azo-coupling reaction were unsuccessful and 8HQ were not bound into the sol-gel, the N/C ratio of the immobilized amine-silane (after hydrolysis of the methoxy-groups and loss of methanol) would be 0.194. The observed N/C ratio for the ligand immobilized in the silica sol-gel material was 0.23 ($\pm$ 0.01), which is indistinguishable from the theoretical value for complete conversion of the phenyl-amine silane to the azo-linked 8HQ ligand. The homogeneous metal-ion binding response of the templated material is consistent with this observation (see below).

Preparation of buffers. The buffer system for these experiments should have negligible fluorescence, minimal complexation with metal ions, spectroscopic transparency, and known ionic strength. To meet these criteria, buffers were composed of hydrochloric acid, chloroacetic acid (pK_A = 2.88 [31]), acetic acid (pK_A = 4.76 [31]), and potassium phosphate (pK_{A2} = 7.21 , pK_{A3} = 12.33 [31]) titrated with sodium acetate and sodium chloroacetate. Potassium chloride was added to produce a 0.1 M constant ionic strength. The pH of each solution was verified at 23 ^{O}C with a pH meter.

Raman spectroscopy measurements. The Raman spectrometer system used for this study is shown in Figure 2 A, and is based on a PI-200 HP Raman instrument (Process Instruments Inc.). The instrument incorporates a frequency-stabilized, narrow-linewidth 785 nm diode laser; a temperature-controlled (F/1.4) fiber-coupled spectrograph, an Andor CCD camera TE-cooled to -75 ^{o}C; and PROspect^{TM} data acquisition software. The diode laser output is coupled to a fiber optic probe from InPhotonics, which consists of a single 200-μm excitation fiber, with built-in filtering to remove unwanted Raman scattering and fluorescence generated within the excitation fiber from the fiber output. The probe uses a 5-mm focal length lens for delivering the laser excitation source to the sample and for collection of the Raman scattered light. This back scattering collection geometry allows simple alignment and high efficiency due to the overlap between the excitation and collection cones. A single collection 400-μm fiber is

used to return scattered Raman light to a 27-optical fiber round-to-slit converter at the spectrograph. Raman scattered light is collimated with a lens and dispersed with a conventionally ruled grating (1200 line/mm), and focused onto the CCD array detector with a second lens. Samples were typically exposed to 250 mW of excitation power, and scattering was integrated for 20 s.

For acquiring Raman spectra under continuous-flow conditions, the output from the Raman probe was focused onto a microflow cell shown in Figure 2B. The microflow cell was a modified stainless steel ¼-in. Swagelock Tee, where one end of the cell was milled off and a 0.1-in. quartz window was epoxied onto the modified end. The cell was assembled by inserting a polished 0.075-in. inner diameter tubing and pressing it up against the quartz window. The connectors on the ends of the Tee held these parts in place, and the side arm of the Tee was used as the solution outlet. The small diameter tubing was then filled with 50 mg of dry sol-gel material and connected to the flow system. A phosphate buffer solution (pH 7.0) flowed through the sample at a rate of 2 mL/min with the aid of a syringe pump (Harvard Apparatus, model PHD 2000) to pack the sol-gel material up against the quartz window. Changes in the Raman scattering were monitored to follow the progress of packing the sol-gel, and typically, the time required for the Raman signal to reach a steady level was ~15 min.

For acquiring Raman spectra in a batch mode experiments to monitor the titration of the templated 8HQ with variable amounts of copper ion, the Raman probe was focused onto the bottom of a quartz cuvette (Figure 2C). The titration was carried out with 200 mg of templated ligand sol gel, suspended in 2 mL of solution and reacted with aliquots of 0.4 M copper-ion solution. After each addition of copper ion, the cuvette was sonicated for 30 minutes to promote mixing and then placed into the focus of the fiber optic probe.

Data analysis. Prior to data analysis, the observed Raman spectra were baseline-corrected by subtracting a 16-point cubic spline from each spectrum. Care was taken to make

sure that all of the 16 points, used to determine the baseline level, were not located within any Raman bands. Classical least-squares regression analysis was employed to test complexation models and to resolve the spectra of the different ligand components. Raman spectra were collected during a series of different runs at constant metal-ion concentrations and variable pH, or constant pH and variable metal-ion concentrations. The spectra from the different runs were collected into the columns of the data matrix, **D**, which contains *r* rows that denote the spectral wavenumber dimension and, *c* columns, which denote the different samples at varying conditions. For any given wavenumber shift, the total Raman scattering intensity can be expressed as the product of the spectral and concentration behaviors of the *n* components (ligand forms) in the sol-gel:

$$D = A * C \quad \textbf{(1)}$$

where **A** is an *r x n* column matrix of *n* pure-component Raman spectra and **C** is an *n x c* row matrix comprising the concentration profiles of each component during a pH titration or metal-ion binding experiment. The determination of the number of components located inside the data matrix during a run was conducted with factor analysis approach developed by Malinowski [32,33]. A covariance matrix, $\mathbf{Z=D^TD}$, was calculated and diagonalized, and a variance ratio or *F* test [34] was applied to the reduced eigenvalues (REV) of the covariance matrix, **Z**. For cases in this study, the numbers of significant components, *n*, were always two or three, and the pure component spectra, **A**, were always available at the concentration extremes of the different data sets. A least-squares estimate of the corresponding concentration profile, $\hat{C}$, can be obtained by left-multiplying the data matrix D by the pseudoinverse of the matrix **A** [35,36]:

$$\hat{C} = [AA^T]^{-1}A^TD \quad \textbf{(2)}$$

The least-squares projected concentration profiles derived from the data, $\hat{C}$, are compared graphically with the optimized concentration model, **C**, where the algebraic solution for the

model is found using Maple version 5. The parameters in the model are varied to determine the minimum of the error surface matrix, χ^2, where χ^2 is the sum of squares of the residuals, $\chi^2 = (1/\sigma^2) \sum (\hat{\mathbf{C}}-\mathbf{C})^2$. The estimated uncertainties for the different parameters in the model were determined by mapping the χ^2 surface to within a 15% range of the best fit of the parameter, p, and the error surface is normalized to its minimum value. Next the curvature of the χ^2 surface is fit to a quadric equation, and the variance in the parameter is then determined by the following expression $\sigma_p^2 = 2/(\delta \chi^2/\delta p^2)$ [37,38]. Replicate measurements resulted in parameter values that were within the uncertainties estimated from the curvature of the error surface. The modeling of the spectroscopic baseline, regression analysis, and determination of parameter uncertainties were computed in MATLAB v5.0 (Mathworks).

RESULTS AND DISCUSSION

Raman spectra of various forms of the metal-ion templated 8HQ ligand. The first investigation was to determine whether the immobilized 8HQ ligand had been correctly assembled into the sol-gel matrix. Previous Raman spectroscopy studies of 8HQ immobilized onto the surface of silica gel [15,16] showed that the various forms of the immobilized ligand had distinct Raman spectra that could be utilized to determine the relative abundance of these ligand forms on the silica surface. From the concentrations of the ligand immobilized in the sol-gel matrix (see above), a 50-mg sample corresponds to ~1.25 μmol of the ligand in the flow cell. The small amount of ligand is helpful in achieving equilibrium with reasonable volumes of low concentration solutions, typically of trace level preconcentration and analysis.

Spectra of the copper-complexed, protonated, neutral, and anionic forms of the templated 8HQ were obtained and compared to previous spectroscopic studies of the same ligand immobilized onto a silica surface (See Figure 3). The copper-complexed form of the ligand was generated by passing 60 mL of a pH 5.5 acetate buffer containing 42 μM Cu^{2+} (100% excess) through the flow cell. The protonated form of the ligand was obtained by flushing the sample with 0.1 M HCl. The neutral form of the ligand was generated by rinsing the sample with acetate buffer, pH 5.5; finally the anionic form was obtained by flushing the sample with a pH 10.6 phosphate buffer. One can observe in Figure 3 the spectral similarities with previous results [16], indicating that the templated ligand in the sol-gel matrix responds similarly to changes in solution conditions as the same ligand immobilized onto a silica-gel surface. Some small differences between the spectra arise from the different excitation wavelength (647.1 nm) used to acquire the previous results [15,16] where the tail of the electronic absorption band in the visible leads to resonance enhancement for specific modes of vibration.

The distinct spectral features that allow the different forms of the ligand to be distinguished arise from changes in the tautomeric form of the ligand [15,16]. The strong 1400-

1450 cm^{-1} symmetric $\nu_{N=N}$ azo stretching vibrations [39] can be observed at ~ 1430 cm^{-1} for the complexed, neutral, and anion forms of the ligand. Other evidence of the azo tautomer in these three forms of the ligand are the ~ 1140 and 1190 cm^{-1} bands corresponding to the ν_{C-N} azo symmetric stretch and ν_{C-N} symmetric bend, respectively [39]. The intense peak at 1377 cm^{-1} in the anion and copper complexed form is associated with the ν_{C-C} mode of the quinoline ring, and it appears as a shoulder in both the protonated and neutral forms [40]. The strength of the $\nu_{N=N}$ azo band in the copper-complexed ligand indicated that the metal-ion coordination does not involve the N atoms of the azo bridge, but the stronger ring nitrogen and phenolic oxygen in the quinoline ring.

An indication of the hydrazone tautomer [15,16] is observed by the large 1283 cm^{-1} ν_{C-C} in-plane stretching band that is associated with this form of the ligand. This band is only observed in the protonated and neutral forms of the ligand, where the accompanying decrease in the azo band intensity is consistent with forming the hydrazone tautomer [40]. The increase in intensity of the ν_{C-C} stretching vibrations at 1595 cm^{-1} in the protonated and neutral forms is also consistent, since this band is stronger in the hydrazone tautomer [40]. Further evidence of the hydrazone tautomer in both the protonated and neutral forms of the ligand can be found in the shoulder at ~1620 cm-1, which has been assigned to $\nu_{C=C}$ and $\nu_{C=N}$ in hydrazones of azonaphthols and azoquinolines [40]. These results show that the anion and complexed forms of the ligand are predominately the azo tautomer, the protonated ligand is dominated by the hydrazone tautomer, while the neutral ligand exists in both tautomeric forms.

Raman spectroscopy of CuQ_2 and CuQ^+. In free solution, metal-ion complexation by 8-hydroxyquinoline occurs predominantly with a stoichiometry that is equivalent to the metal ion charge [11]. One difference between solution-phase and surface-immobilized 8HQ ligands is that the immobilized ligands are generally spaced too far apart to form higher order complexes, and the ratio of immobilized 8HQ ligands to complexed metal ions does not exceed 1:1 [15].

The relative low surface coverage of previously silica immobilized 8HQ ligands [10,13,15,16] results from an inefficient synthesis where first a linker is attached onto the silica surface and then the ligand is bound to the linker. In contrast, this work first creates a bis-ligand complex with a ligand that can already bind to silica, and then synthesizes a porous sol-gel matrix around the complex to immobilize it onto a silica surface. This technique should preserve the geometry of the bis-ligand complex and allow formation of higher-order complexes defined by the following reactions:

$$Cu^{2+} + Q^{-} \xleftrightarrow{K_1^o} CuQ^{+} + Q^{-} \xleftrightarrow{K_2^o} CuQ_2 \qquad (3)$$

Our first goal was to ascertain whether there were discernable spectral differences between the bis-ligand and mono-ligand complexes. This study was conducted by loading the microflow cell with 50 mg of freshly templated sol-gel material which corresponds to ~1.25 μmol of 8HQ ligands in the sample (see above). Initially, the ligands should be in a 2:1 ratio with the bound metal-ion that was present during the synthesis; the addition of excess copper ions should form mono-ligand complexes having a 1:1 ligand:metal ratio. This displacement of a ligand from the initial bis-ligand complex by the addition of excess copper ion is apparent by rewriting the reactions of Equation 3 in the following order:

$$Cu^{2+} + 2Q^{-} \xleftrightarrow{K_1^o K_2^o} CuQ_2 + Cu^{2+} \xleftrightarrow{K_1^o / K_2^o} 2CuQ^{+} \qquad (4)$$

Previous studies of solution-phase complexation [11,29] have shown that 1:1 complexes are more stable in the presence of excess metal ion, since the first formation constant K_1^O is greater than the second-step formation constant K_2^O by at least a factor of 10. To generate the lower-order complex, the sample was flushed with 90 mL of a buffered pH 8 solution containing 10 μM Cu^{2+}. The solution was passed through the material at a flow rate of 0.5 mL/min, and Raman spectra were collected every 40 s. These conditions introduce an

additional 0.9 μmol of copper ion into the sol-gel matrix, where only ~0.63 μmol of ligand would be available to complex the additional Cu^{2+} ions. Modeling the equilibria for the forms of the ligand [11,29] showed that, under these experimental conditions, only the bis- and mono-ligand:metal complexes should be present in any significant concentrations, and all other forms of the ligand will be negligible. Figure 4 displays a sample of the Raman spectra acquired during the run, with the bottom spectrum corresponding to time 0 (2:1 ratio) and the top spectrum corresponding to the end of the series (1:1 ratio). The dominant spectral differences between the two complexes are observed in an initially strong band at 1288 cm^{-1} that shifts to 1280 cm^{-1} upon the addition of Cu^{2+}. Other features that change with increasing Cu^{2+} are a decrease in the 1482 cm^{-1} band and the reduction in the initial background between 1100 and 1225 cm^{-1} spectral region. Factor analysis was able to determine that this data set can be described by two independent components, which should correspond to bis- and mono-ligand complexes; continued flushing of additional copper ions through the sample did not result in any further spectral changes. Spectra at the beginning and end of the run were taken as the pure component spectra (Figure 5A), and least-squares analysis was used to determine the concentration profile of each component versus the addition of Cu^{2+} shown in Figure 5B.

The concentration profile shows that the formation of the 1:1 complex reaches equilibrium after ~ 140 min, corresponding to 0.7 μmol of copper ion. This is quite a reasonable result since it corresponds to just over half of the 1.25 μmol templated ligand in the sample. The slight excess of copper ion required to complex to the templated ligand during the titration could result from the time required for the Cu^{2+} ion to penetrate into the pores of the sol-gel matrix and interact with the immobilized 8HQ; in addition, a slight excess concentration could be required to drive the equilibrium to the monomeric ligand complex.

Proton-transfer equilibrium constants of the templated ligand. Determination of the acid dissociation steps of the templated 8HQ ligand is important for understanding metal-ion

complexation since the metal binds to the anion form of the ligand, and the activity of the anion form varies with pH.

$$HQH^{+} \xleftrightarrow{K_{A1}} H^{+} + HQ \xleftrightarrow{K_{A2}} H^{+} + Q^{-} \quad (5)$$

The protonated form of the ligand dominates below a pH of ~ 3.5 [13,16]; above a pH of ~ 10 [16,41], the ligand is in the anion form, and at intermediate pH values, the neutral form is dominant. To determine the acid dissociation constants, the sample cell was filled with 50 mg of templated-ligand sol-gel, and then the sample was washed with 0.1 M HCl to remove the complexed copper ions that were present during the synthesis. The sample was then flushed with buffered solutions of increasing pH for one hour each over the range of pH = 1.0 to 5.3, and Raman spectra were acquired at each pH (Figure 6). Changes in band intensities can be observed versus pH; scattering from the protonated form of the ligand decays with increasing pH, while bands from the neutral form rise with increasing pH. Using spectra of the protonated and neutral forms of the ligand at the pH extremes (see above), a multidimensional least-squares analysis (Equation 2) was used to determine the relative concentrations of each species versus pH, and the results are plotted in Figure 7A. The pK_{A1} was determined from the concentration profiles by combining a normalized conservation of mass expression for the two forms of the ligand:

$$[HQH^{+}] = 1 - [HQ] \quad (6)$$

with the proton-transfer equilibrium expression:

$$K_{A1} = \frac{[HQ]\ a_H \exp(-F\Psi_X / R\,T)}{[HQH^{+}]} \quad (7)$$

where the proton activity at the interface is not the same as in bulk solution, a_H, due to the repulsion or attraction of ions at the interface by the surface potential ψ_x; corrections to the

interfacial ion activity are provided by the exponential term (the Boltzmann equation [13,16,42]) where F and R are Faraday's constant and the gas constant, respectively. Values for the surface potential were previously measured for 8HQ-derivatized, 5-µm particle diameter silica gel, which could be dispersed in aqueous solution [16]. Determination of the first acid dissociation constant was accomplished by solving Equations 6 and 7 for HQ and HQH^+ using a series of K_{A1}'s, and the least-squares best fit to the pH-dependent concentration profiles resulted in $pK_{A1} = 2.6 \pm 0.25$. The quality of fit to the spectral concentration profiles shows good agreement with Equation 7, and the result is within the uncertainty of the previously reported pK_{A1} of silica-surface immobilized 8HQ [16].

The second acid dissociation step of 8HQ was determined from Raman scattering of the neutral and deprotonated forms of the ligand over a pH range from 6.1 to 10.3. Using the predetermined pure component spectrum, a least squares analysis (Equation 2) was used to determine the concentration profiles for both the neutral and anionic form of the immobilized ligand versus pH. The results are plotted in Figure 7B, along with the least-squares best fit concentration profiles of the neutral and anionic forms of the ligand from the following two equations.

$$[HQ] = 1 - [Q^-] \tag{8}$$

and

$$K_{A2} = \frac{[Q^-]\ a_H \exp(-F\Psi_X / R\,T)}{[HQ]} \tag{9}$$

The best-fit expressions resulted in a pK_{A2} of 8.75 ± 0.2, which is equivalent within errors to the previously reported pK_{A2} for silica-surface immobilized 8HQ [16].

Copper-ion binding by templated and non-templated 8HQ. While the acid/base behavior of the metal-ion templated 8HQ-silica sol gel is equivalent to silica surface-immobilized ligands, the equilibrium constants for metal-ion binding should be different. The Cu^{2+} binding

reaction by the immobilized ligand can be investigated by a spectrophotometric titration, monitoring the concentration profiles of the different ligand forms during the reaction. The spectra for CuQ^+ and CuQ_2 are highly overlapped, so that the reaction conditions (ligand and metal concentration, and pH) must be carefully controlled to ensure that variation of the species of interest are observed. Variation from other forms of the ligand could dominate the residual error in fitting the data and lower the sensitivity for resolving the first and second Cu^{2+} binding steps. To avoid varying the unbound forms of the ligand, an acid-base titration was not used, and the pH was held constant. By utilizing a known amount of templated ligand at a constant pH and only varying the amount of Cu^{2+} added to the sample, a data set can be created where only the metal-complex forms of the ligand are changing. To determine the appropriate solution conditions, a model was developed to describe the relative concentration profiles for the first and second binding constants of the ligand. The equilibrium complexation model for the metal complexes formed in the reactions of Equation 3 and 5 employed a normalized mass balance expression for the ligand concentrations:

$$1 = [HQH^+] + [HQ] + [Q^-] + [CuQ^+] + 2[CuQ_2] \tag{10}$$

along with the equilibrium expressions for the metal complexes formed:

$$K_1^O = \frac{[CuQ^+]}{[Q^-] \quad a_{Cu^{+2}} \exp\left(-2F\Psi_X / RT\right)} \tag{11}$$

and

$$K_2^O = \frac{[CuQ_2]}{[CuQ^+][Q^-]} \tag{12}$$

The equilibrium complexation model was solved numerically to predict the expected concentration profiles for each of the 8HQ forms. For an initial estimate of the expected behavior of the system, we utilized a previously determined value of $K_1^O = 4.8 \times 10^8$ for the first

formation constant obtained from the same ligand immobilized onto the surface of a silica particle [16]. The second formation constant was estimated to be $K_2^O \sim 5 \times 10^7$ based on the free solution data that showed a ~tenfold decrease in K_2^O compared to K_1^O for 8HQ in solution [11,29,43]. Using these estimates for K_1^O and K_2^O and the measured values for the proton transfer equilibrium constants (above), the complexation model was solved numerically and the resulting concentration profiles were evaluated to find appropriate reaction conditions where the 8HQ ligand would be found only in its neutral, 1:1 and 2:1 ligand:metal complexed forms.

This initial modeling showed that a constant pH of 5.7 solution containing a known amount of the templated ligand with increasing amounts of Cu^{2+} would produce the desired forms of the ligand. To generate this data set, we utilized the batch-mode titration (Figure 2c) by placing 200 mg of 8HQ templated sol-gel into a cuvette containing 2 mL of a pH 5.7 buffered solution. The ligand had been previously washed with HCl to remove all of the initially complexed Cu2+ ions, and then rinsed throughly with a pH 5.7 buffer to produce the neutral form. The stepwise titration was then conducted by adding increasing amounts of metal ion by additions of a 125 μM Cu2+ solution that was buffered to a pH of 5.7.

Using the elemental analysis results for the templated 8HQ, one can estimate that the 200 mg of the sol-gel material corresponds to ~ 5.0 μmol of the templated ligand. Raman spectra were collected after each titration, and the observed spectra are displayed in Figure 8 with offsets to demonstrate the spectral changes that occurred during the titration. The bottom spectrum corresponds to the neutral form of the ligand before any metal was added, and the top spectrum corresponds to the 1:1 ligand:metal ratio. In the 1275 to 1300 cm^{-1} spectral region of the data, the 1288 cm^{-1} band associated with the CuQ_2 form of the ligand initially increases upon the addition of metal ions; at ligand to metal ratios above 1:0.5, this band decreases indicating that the templated CuQ_2 form is being converted from the 2:1 to the 1:1 complex. The top three spectra, corresponding to the most concentrated Cu^{2+} solutions, show no scattering at 1288 cm^{-}

[1] which indicates that the CuQ_2 form is no longer present and the CuQ^+ form dominates above a ligand-to-metal ratio of 1:2. The number of components in the data matrix was determined by factor analysis [32,33] to be 3, which should correspond to the neutral, and 2:1 and 1:1 complexed forms, respectively.

To determine the concentration profiles for each of the different species during the titration, we used the previously determined pure component spectra, which are plotted in Figure 9, and each of these spectra were obtained by inserting 200 mg of the templated sol-gel material inside a quartz cuvette containing 2 mL of pH 5.7 buffer solution. The spectrum of the neutral form of the ligand was obtained by flushing a freshly templated sol-gel sample with HCl solution to remove the complexed Cu^{2+}, and then equilibrating the sample with a pH 5.7 buffer. The CuQ_2 spectrum was acquired from a freshly prepared templated sol-gel, which initially templated the ligand into the 2:1 ligand-to-metal complex. The spectrum of the CuQ^+ form was generated by placing 200 mg of freshly prepared templated sol-gel into the sample cell and flushing with 30 mL of a 166 μM Cu^{2+} solution (100 times excess). Using these pure-component spectra as factors, a classical least-squares analysis of the component concentrations was performed using Equation 2. The estimated CLS concentration profile, $\hat{\mathbf{C}}$, for the CuQ_2 form of the ligand will be different from the equilibrium concentration model (discussed above), since $\hat{\mathbf{C}}$ only determines the individual spectral concentration profiles and does not include the normalized mass balance expression shown in Equation 10. The equilibrium model was derived so that each CuQ_2 form is counted as a single bis-complex. However, the estimated CLS concentration profile fits the Raman scattering from both ligands that are complexed to a single Cu^{2+} ion and so it will produce a concentration profile that is ~2-times larger than predicted in the equilibrium concentration model due to the higher scattering cross section of the bis-ligand complex. The CLS-estimated CuQ_2 concentration profile was, therefore, divided by 2 to be consistent with the optimized concentration model.

Figure 10A shows the resulting Cu^{2+} dependent concentration profiles of the neutral, 2:1 complexed, and 1:1 complexed forms of the templated ligand for a pH 5.7 buffered solution. The free, neutral ligand shows a linear decrease with increasing Cu^{2+} concentrations that reaches the baseline once the ligand to metal ratio reaches 1:0.5. In contrast, the CuQ_2 form of the ligand rises linearly with Cu^{2+} concentration until all of the ligands are complexed, which is indicated by the concentration profile reaching 0.5. Interestingly the 1:1 ratio does not start to appear until the concentration of metal ions is greater than half of the ligand concentration indicating that the templated 2:1 complex forms first, and an excess amount of Cu^{2+} is required to produce the 1:1 complex. To determine the first- and second-equilibrium constant, a range of K_1^O and K_2^O values were modeled numerically, and their results were tested for their fit to the measured concentration profiles in Figure 10A. The sums of squares of the residuals were determined in the range of the optimum for each parameter and are plotted in Figure 10B. The nearly flat error surface in the K_2^O dimension for increasing values of the parameter indicates that we can only determine the lower bound for K_2^O. The best fit results corresponded to K_1^O = 4.5 (± 1.8) x 10^8 and $K_2^O \geq$ 4.0 (± 0.8) x 10^8. The first Cu^{2+} binding equilibrium constant is within error bounds for the identical surface immobilized ligand (K_1^O = 4.8 x 10^8) [16]. While the estimated second binding constant is only a lower bound for its actual value, it is clear that the actual value is *not* an order-of-magnitude smaller than the first binding constant, as expected from free-solution binding studies [11,43]. From the results, there is strong evidence that the free energy available for binding the second ligand within the templated material is comparable to or greater than the first ligand. This could be due to the nearly *optimal location of the 2nd ligand* for binding based on the templating that is done during this synthesis. This optimal geometry would greatly reduce the *entropy cost*s for binding a 2nd ligand since its location is already constrained by the structure of the surrounding sol-gel material. The entropy costs were paid at the time that the material is synthesized, which increases the free energy available for

binding a second ligand.

Final experiments were carried to verify that the above results were indeed due to the templating of a 2:1 complex in the sol-gel structure. Modifications were made to the synthesis to produce a material where only half of the immobilized ligands could be templated and also a sol-gel matrix where none of the ligands would be templated. The only alteration to the synthesis was the amount of Cu^{2+} that was introduced into the pH 8 solution prior to the introduction of tetraethoxysilane to produce the sol gel. Originally, we had added sufficient Cu^{2+} so that the ligand to metal ratio was 2:1. To template only half of the ligands 0.01 mmol of cupric chloride was included into the solution containing 0.04 mmol of the ligand. This ratio was chosen so that one-half of the ligands would be available to form a CuQ_2 complex with the copper ion, while the remaining excess ligands would be free of copper ion during the synthesis. The non-templated form of the ligand was created by adding no metal ions to the original synthesis. Except for the changes in the amount of Cu^{2+} present during the formation of the sol-gel matrix, no other changes were made in the above material preparation procedure. Raman spectra from the various forms of the ligand for each of these materials were obtained by using the batch mode technique described above, by placing 200 mg of 8HQ templated sol-gel into a cuvette containing 2 mL of a pH 5.7 buffered solution and stepwise increasing the amount of Cu^{2+}. Factor analysis reported in three independently varying spectral components for the half-templated sol-gel, but only two components for the sol-gel containing no templated ligands. Using the previously determined pure component spectra in Figure 9, a least-squares analysis was used to determine the concentration profiles for the neutral, 2:1 complexed, and 1:1 complexed forms of the half-templated and non-templated ligand materials. Figure 11B and C shows the concentration profiles for the half-templated and non-templated ligands, respectively, which can be compared with results from a sol-gel with all of the ligands templated (Figure 11A).

There are two significant indications that we have successfully templated half of the ligands in the sol-gel characterized in the middle-panel of Figure 11. First, the peak in the CuQ_2 concentration profile for the half-templated ligands is approximately half of the maximum when all of the ligands were templated (Figure 11A); both of these concentration profiles reach a maximum when the added metal ions are about ½ of the ligands. Secondly, the initial rise in the 1:1 complex occurs at a lower metal-ion concentration indicating that a significant fraction of the ligands are not present in a bis-complex templated form. Figure 11C shows the concentration profiles for the non-templated sol-gel material, where the concentration profile for the CuQ_2 form never rises above the baseline during the entire Cu^{2+} titration. One can also notice that there is no initial concentration delay with the onset of forming the 1:1 ligand:metal complex. These two factors indicate that none of the ligands have been templated to form CuQ_2 complexes on the surface, and one can only observe the neutral and CuQ^+ forms of the immobilized ligand in these spectra.

Summary. Metal-ion templating in a sol-gel synthesis has been used to template multi-ligand 8-hydroxyquinoline binding sites in porous silica structures. The proton-transfer equilibrium constants and first-ligand binding equilibrium constant to Cu^{2+} for the metal-ion templated silica were equivalent to surface-immobilized 8HQ on silica gel. The second ligand binding constant to Cu^{2+}, however, was comparable to the first ligand binding constant, which differs from free-solution behavior, where an order-of-magnitude smaller value is expected. The free energy available for binding the second ligand within the templated material is comparable to the first ligand, probably due to smaller entropy cost for binding the second ligand and its nearly optimal location for binding, based on the templating that is done during the synthesis. The metal-ion concentration responses of sol-gels prepared with varying amounts of metal ion during the syntheses indicated control over the fraction of templated binding sites. Despite the possible variation in the local structure of the complexation sites in the silica material, the

concentrations of the various forms of the ligand versus pH and metal-ion stoichiometry were well fit by *discrete* proton-transfer and metal-ion binding equilibrium constants. These results indicate that the binding sites within the sol-gel material are energetically homogeneous and not characterized by a broad distribution of ion-binding free energies. This energetic homogeneity could provide selectivity for the particular metal ion used in the initial templating response. Future research will be directed toward the metal-ion selectivity of these structures, where *in situ* Raman spectra will be examined for evidence of strained complexes of mismatched metal ions in the templated materials.

ACKNOWLEDGMENTS

This work was supported in part by the U.S. Department of Energy under Grant DE-FG03-93ER14333.

LITERATURE CITED

1. Bruening, R. L.; Tarbet, B. J.; Krakowiak, K. E.; Bruening, M. L.; Izatt R. M.; Bradshaw, J. S. *Anal. Chem.* **1991**, 63, 1014-1017.
2. Izatt, R. M.; Pawlak, K.; Bradshaw, J. S.; Bruening,R. L.; *Chem. Rev.* **1991**, 91, 1721-1785.
3. Jezorek, J. R.; Tang, J.;Cook, W. L.;Obie, R.; Ji, D.; Rowe, J. M. *Anal. Chim. Acta* **1994**, 290, 303-315.
4. Lessi, P.; Moreira, J. C.; Filho, N. L.; Campos, J. T. *Anal. Chim. Acta* **1996**, 327, 183.
5. Hankins, M. G.; Hayashita, T.;Kasprzyk, S. P.; Bartsch, R. A. *Anal. Chem.* **1996**, 68, 2811-2817.
6. Feng, X.; Fryxell, G. E.; Wang, L.-Q.; Kim, A. Y.; Liu, J.; Kemner, K. M. *Science **1997**,* 276, 923-926.
7. Hill, J. M. *J. Chromatogr.* **1973**, 76, 455-458.
8. Jezorek, J. R.; Freiser, H. *Anal. Chem.* **1979**, 51, 366-373.
9. Marshall, M. A.; Mottola, H. A. *Anal. Chem.* **1983**, 55, 2089-2093.
10. Marshall, M. A.; Mottola, H. A. *Anal. Chem.* **1985**, 57, 729-733.
11. Starý, J.; Zolotov, Y. A.; Petrukhin O. M. *Critical Evaluation of Equilibrium Constants Involving 8-Hydroxyquinoline and its Metal Chelates*; IUPAC Chemical Data Series No 24; Pergamon Press: Oxford, U.K., **1979**.
12. Howard, M. E.; Holcombe, J. A. *Anal. Chem.* **2000**, 72, 3927-3933.
13. Weaver, M. R.; Harris, J. M *Anal. Chem.* **1989**, 61, 1001-1010.
14. Chow, P. Y. T.; Cantwell, F. F. *Anal. Chem.* **1988**, 60, 1569-1573.
15. Uibel, R. H.; Harris, J. M. *Appl. Spec.* **2000**, 54, 1868-1875.
16. Uibel, R. H.; Harris, J. M. *Anal. Chem.* **2002**, 74, 5112-5120.

17. Kuchen, W.; Schram, J. *Angewandte Chemie* **1988**, 100, 1757-63.

18. Tsukagoshi, K.; Yu, K. Y.; Maeda, M.; Takagi, M. *Bul. Chem. Soc. Japan* **1993**, 66, 114-20.

19. Chanda, M.; Rempel, G. L. *Can. Ind. Eng. Chem. Res.* **1995**, 34, 2574-83.

20. Yoshida, M.; Uezu, K.; Goto, M.; Furusaki, S. *Macromolecules* **1999,** 32,1237 -1243.

21. Prasada Rao, T.; Daniel, S.; Mary Gladis, J. *Trends Anal. Chem.* **2004**, 23, 28-35 (and references therein).

22. Dai, S.; Burleigh, M. C.; Ju, Y. H.; Gao, H. J.; Lin, J. S.; Pennycook, S. J.; Barnes, C. E.; Xue, Z. L. *J. Am. Chem. Soc.* **2000**, 122, 992-93.

23. Burleigh, M. C.; Dai, S.; Barnes, C. E.; Xue, Z. L. *Sep. Sci. Techn.* **2001**, 36, 3395-3409.

24. Dai, S. *Chem. Eur. J.* **2001**, 7, 763-768.

25. He, J.; Ichinose, I.; Kunitake, T. *Chem. Lett.* **2001**, 850-51.

26. Burleigh, M. C.; Dai, S.; Hagaman, E. W.; Lin, J. S. *Chem. Mater.* **2001**, 13, 2537-2546.

27. Stöber, W.; Bohn, E. *J. Colloid Interface Sci.* **1968**, 26 (1), 62-9.

28. van Blaaderen, A.; Vrij, A. *Langmuir* **1992**, 8, 2921-2931.

29. Uibel, R. H.; Harris, J. M. *Anal. Chim. Acta* **2003**, 494, 1005-123.

30. Long, R.; K. Schofield, K. *J. Chem. Soc*. **1953**, 3161-3167.

31. Benyon, R. J.; Easterby, J. S. *Buffer Solutions. The Basics*; IRL Press: Oxford, 1996.

32. Malinowski, E. R. *Factor Analysis in Chemistry*, 3rd ed.; John Wiley and Sons: New York, 2002.

33. Malinowski, E. R. *Anal. Chem.* **1977**, 49, 612-617.

34. Barlow, R. J. *Statistics a Guide to the Use of Statistical Methods in the Physical Sciences*; John Wiley and Sons: New York, 1989.

35. Draper, N. R.; Smith, H. *Applied Regression Analysis*; John Wiley and Sons: New York,

1981.

36. Tauler, R.; Kowalski, B. Fleming, S. *Anal. Chem.* **1993**, 65, 2040-2047.

37. Bevington, P. R. *Data Reduction and Error Analysis for the Physical Sciences*; McGraw-Hill Book Co.: New York, 1992.

38. Philips, G. R.; Eyring, E. M. *Anal. Chem.* **1988**, 60, 738-741.

39. Trotter, P. J. *Appl. Spectrosc.* **1977**, 31, 30-35.

40. Bajpai, P. K.; Pal, B.; Basu Baul, T. S. *J. Raman Spectrosc.* **1995**, 26, 351-361.

41. Kolstad, K.; Chow, P. Y. T.; Cantwell, F. F.; *Anal. Chem.* **1988**, 60, 1565-1569.

42. Adamson, A. W. Physical Chemistry of surfaces, 4th ed.; John Wiley and Sons: New York, 1982.

43. Fresco, J.; Freiser, H. *Anal. Chem.* **1964**, 36, 372-375.

FIGURE CAPTIONS

Figure 1) Synthesis of the sol-gel immobilized templated 8HQ ligand.

Figure 2) A. Raman spectroscopy instrument for monitoring of metal ion complexation to sol-gel immobilized templated ligands. B. microflow cell used to conduct *in situ* analysis of the immobilized ligands. C. batch mode experiment for monitoring the titration of the templated 8HQ with variable amounts of copper ion.

Figure 3) Normalized Raman spectra for the templated 8HQ ligands immobilized into a sol-gel (top spectra), and non-templated 8HQ immobilized onto the surface of silica particles (bottom spectra) [16]. The spectra represent the CuQ^+ complexed (A), neutral (B), protonated (C), and deprotonated (D) forms of the ligand.

Figure 4) Raman spectra from 50 mg of freshly prepared templated 8HQ ligand placed inside the microflow cell that is flushed with 90 mL of a 10 μM Cu^{2+} buffered solution. The bottom and top spectra correspond to the start and end of the experiment, respectively.

Figure 5) A. Raman spectra from the initial (bottom) and final (top) acquisition in Figure 4. The initial spectrum corresponds to the CuQ_2 form of the ligand, while the top spectrum is the CuQ^- form. B. Least-squares optimized $\hat{C}$ matrix (from the data displayed in Figure 4) showing the relative concentrations of the 2:1 and 1:1 ligand:metal complexes in the templated material.

Figure 6) Normalized Raman spectra of sol-gel immobilized 8HQ over a pH range of 1.1 to 5.3, showing the titration of the protonated to neutral forms of the ligand. No Cu^{2+} is present in the solution.

Figure 7) A. Relative concentrations of the sol-gel templated 8HQ in its protonated (squares) and neutral (circles) forms, and the fit to Equations 6 and 7 (full line) over the pH range where the surface potential has been measured [16]. B. concentration profiles of the neutral (circles) and anionic (plus) forms, and the fit to Equations 8 and 9 (full line).

Figure 8) Raman spectra of the metal-ion templated 8HQ sol-gel titrated with varying amounts of copper ion in a buffered pH 5.7 solution. Measurements were made with ligand/metal ratios from 1/0 (bottom) to 1/3.7 (top).

Figure 9) Raman spectra of the neutral 8HQ (bottom), CuQ_2 (middle), and CuQ^+ top) forms.

Figure 10) A. Least-squares optimized $\hat{C}$ matrix (from the data displayed in Figure 8) with the relative concentrations of the templated 8HQ in its neutral (circle), CuQ_2 (plus), and CuQ^+ (square) forms. The data are fit by varying K_1^O and K_2^O values (full lines) using Equations 7 - 12, and the previously determined pK_{A1} and pK_{A2} values. B. Sum of the squares of the residuals for variation of the equilibrium constants, K_1^O and K_2^O.

Figure 11) Least-squares optimized $\hat{C}$ matrix with the relative concentrations of the immobilized 8HQ in its neutral free-ligand (circle), CuQ_2 (plus), and CuQ^- (square) forms. The fully templated 8HQ sol-gel is shown in Panel A, 50% templated 8HQ (Panel B), and no initial templating (Panel C).

Figure 1

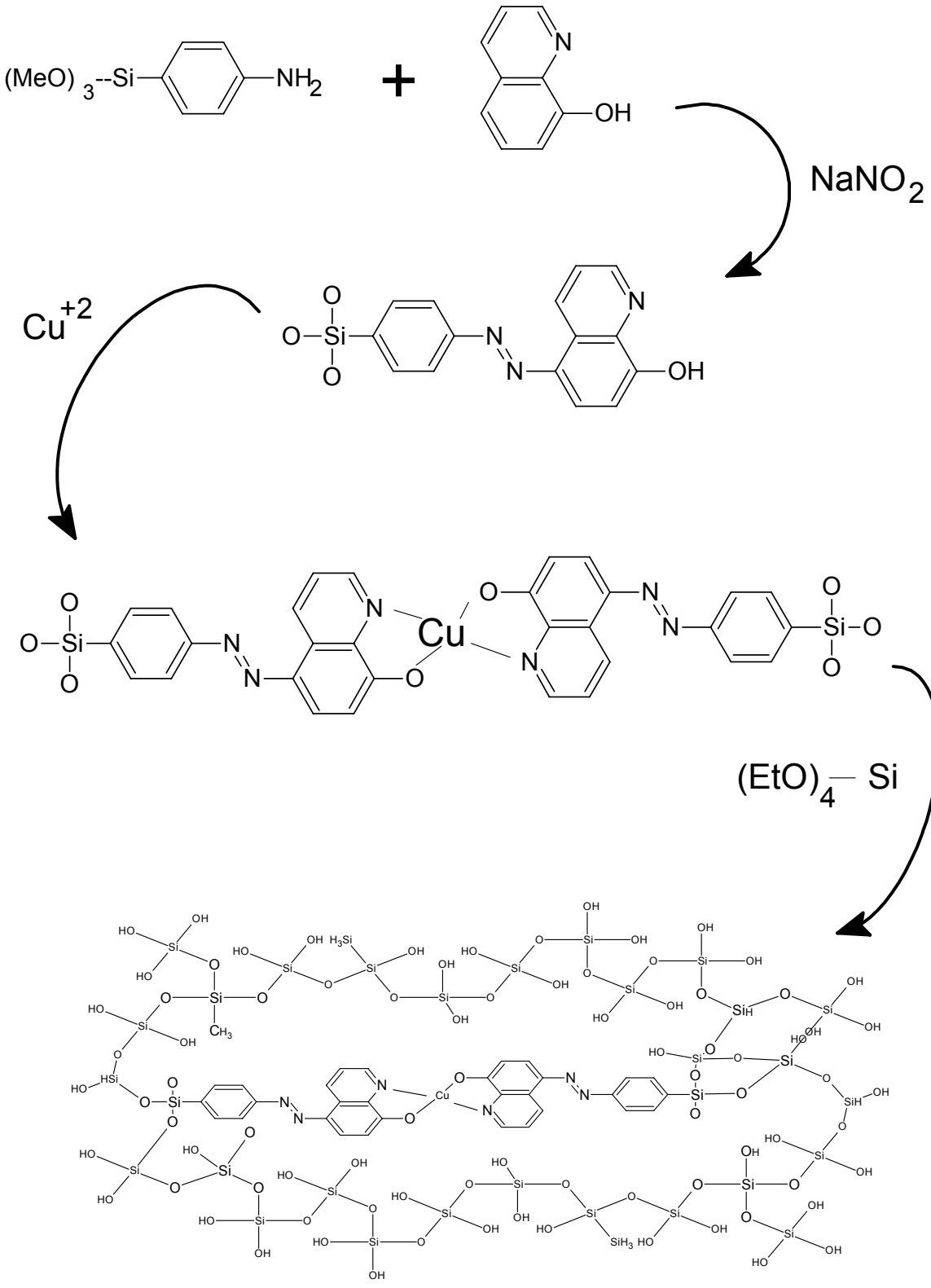

Figure 2

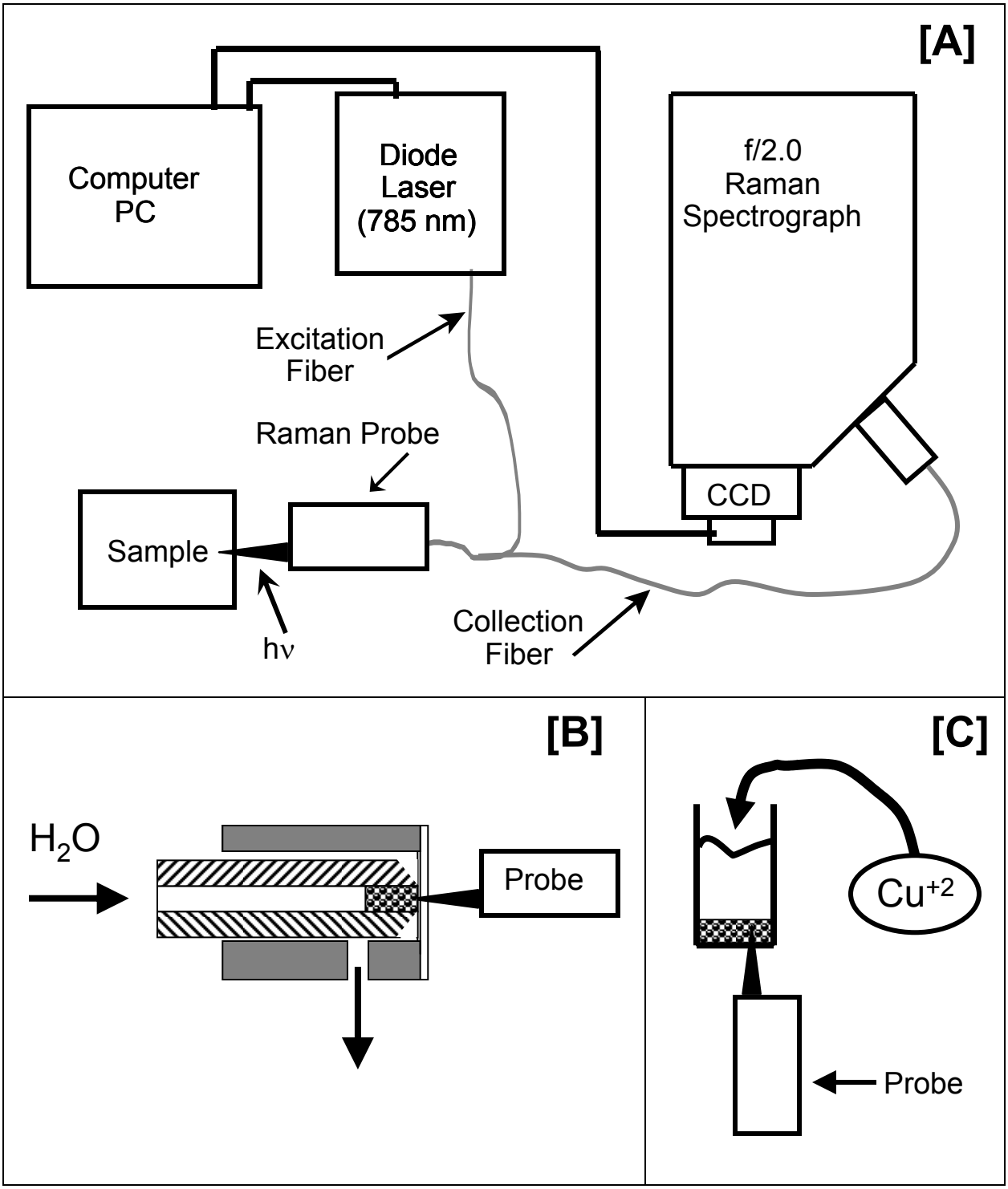
[A]
Computer PC
Diode Laser (785 nm)
f/2.0 Raman Spectrograph
Excitation Fiber
Raman Probe
CCD
Sample
hν
Collection Fiber
[B]
H2O
Probe
[C]
Cu+2
Probe

Figure 3

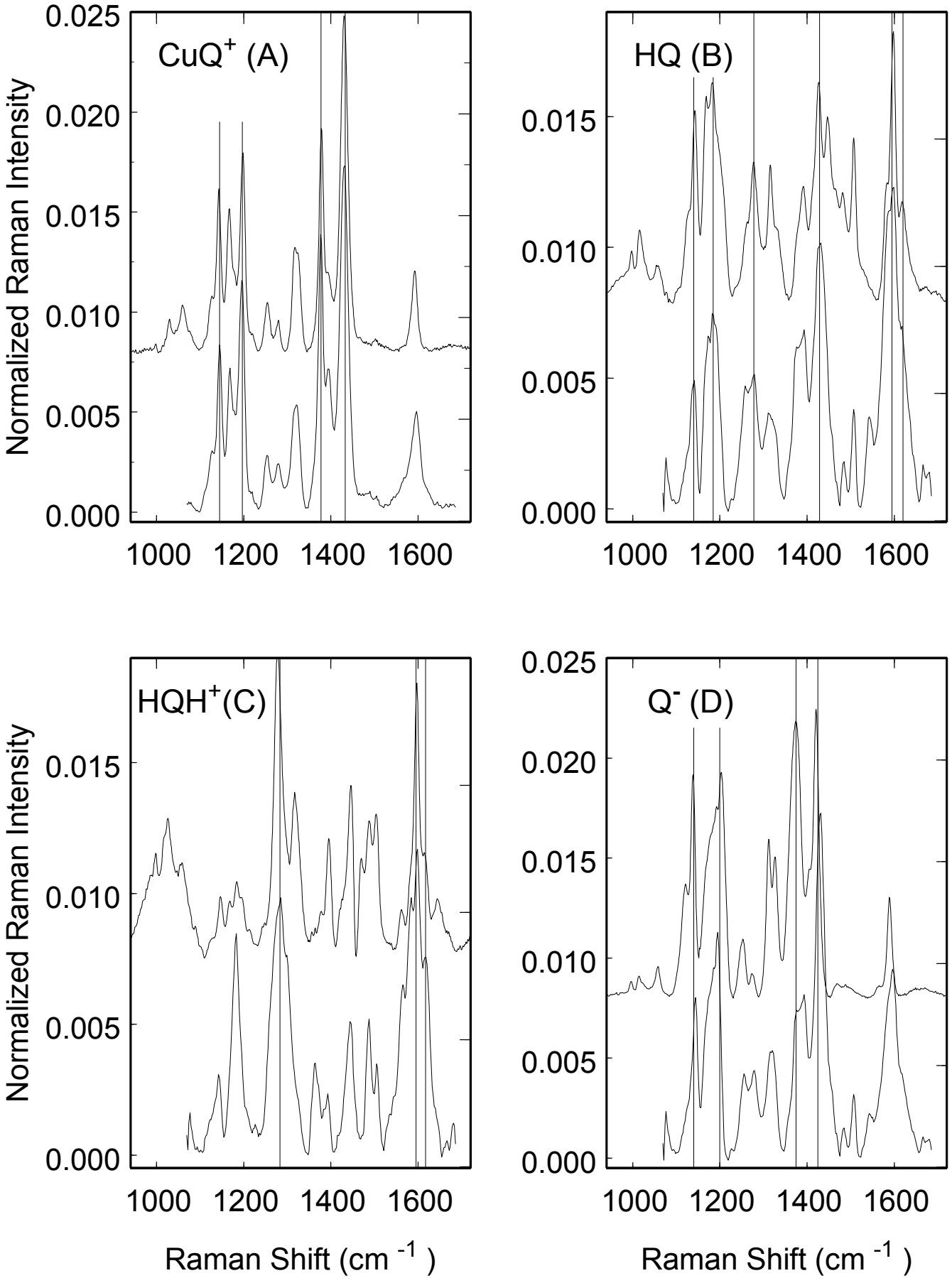
CuQ+ (A)
HQ (B)
HQH+(C)
Q- (D)
Normalized Raman Intensity
Raman Shift (cm -1)
0.025
0.020
0.015
0.010
0.005
0.000
1000
1200
1400
1600

Figure 4

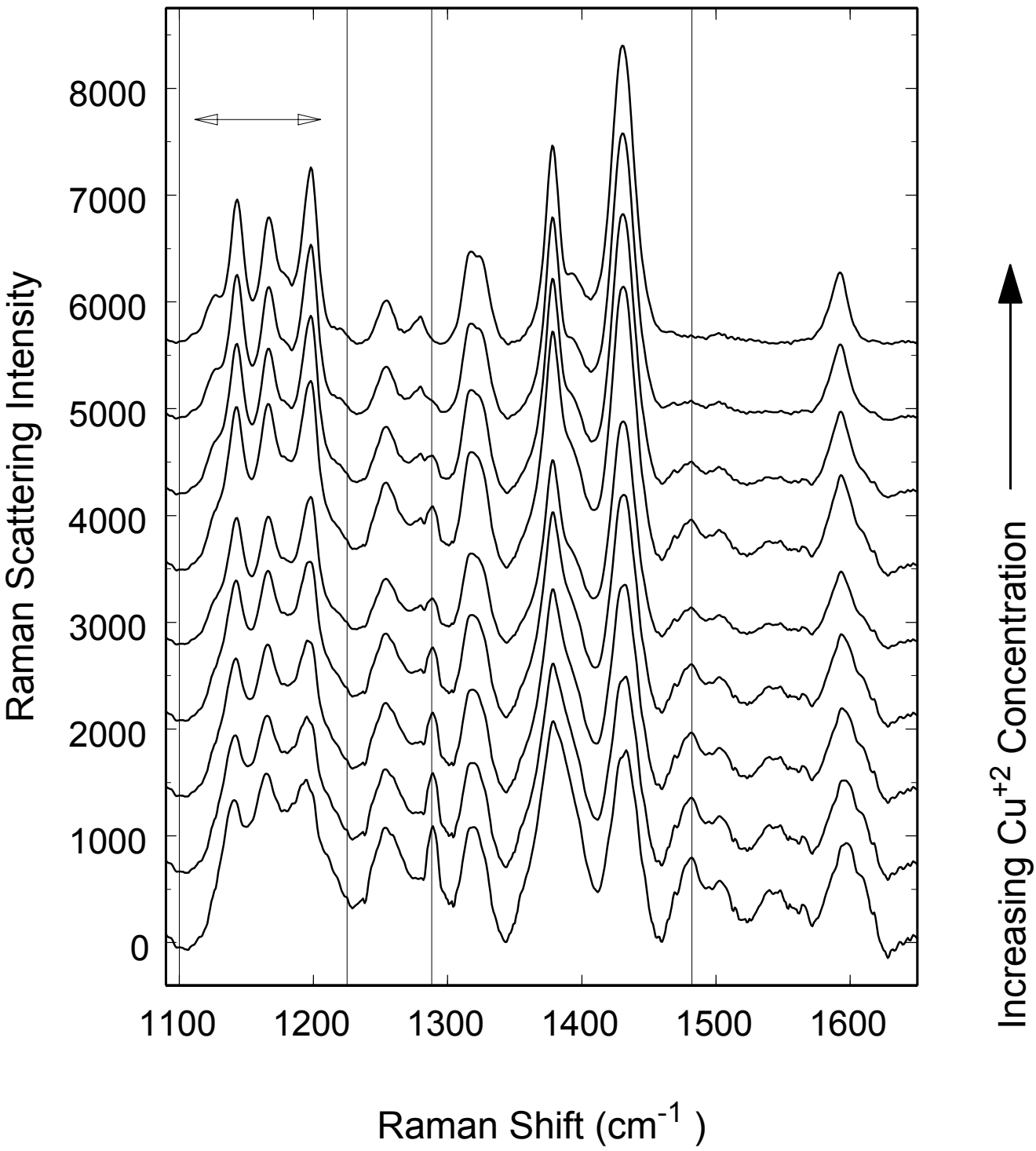
Raman Scattering Intensity
8000
7000
6000
5000
4000
3000
2000
1000
0
1100
1200
1300
1400
1500
1600
Raman Shift (cm-1)
Increasing Cu+2 Concentration

Figure 5

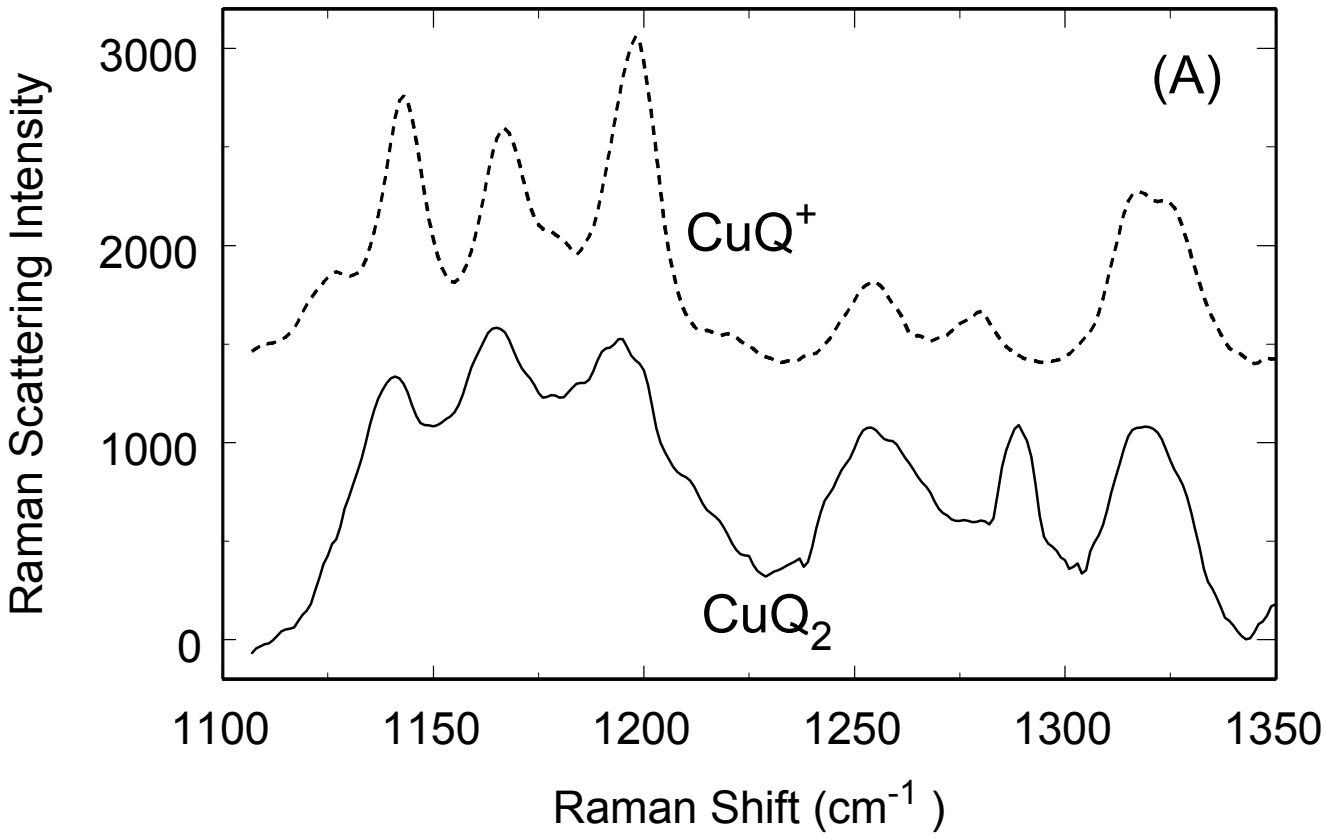
Raman Scattering Intensity
3000
2000
1000
0
(A)
CuQ+
CuQ2
1100
1150
1200
1250
1300
1350
Raman Shift (cm-1)

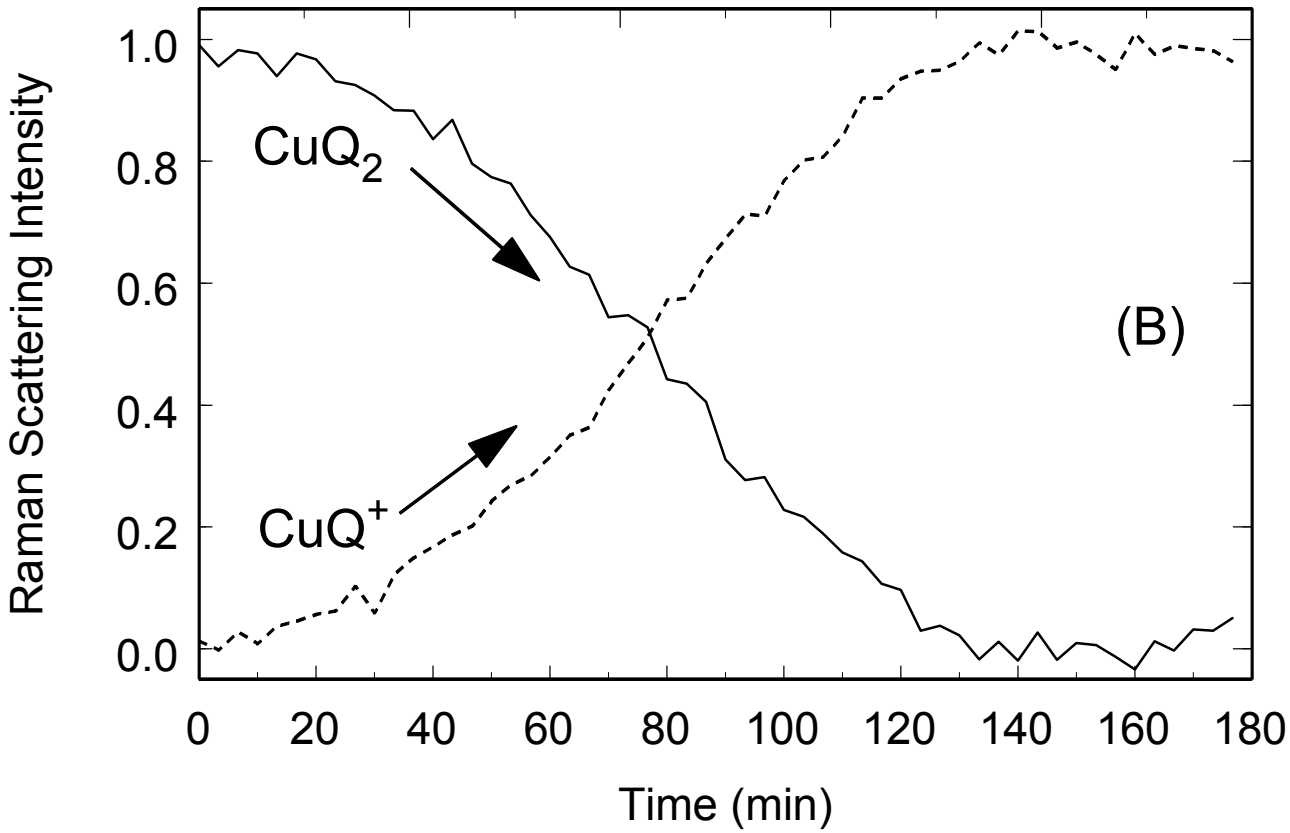
Raman Scattering Intensity
1.0
0.8
0.6
0.4
0.2
0.0
CuQ2
CuQ+
(B)
0
20
40
60
80
100
120
140
160
180
Time (min)

Figure 6

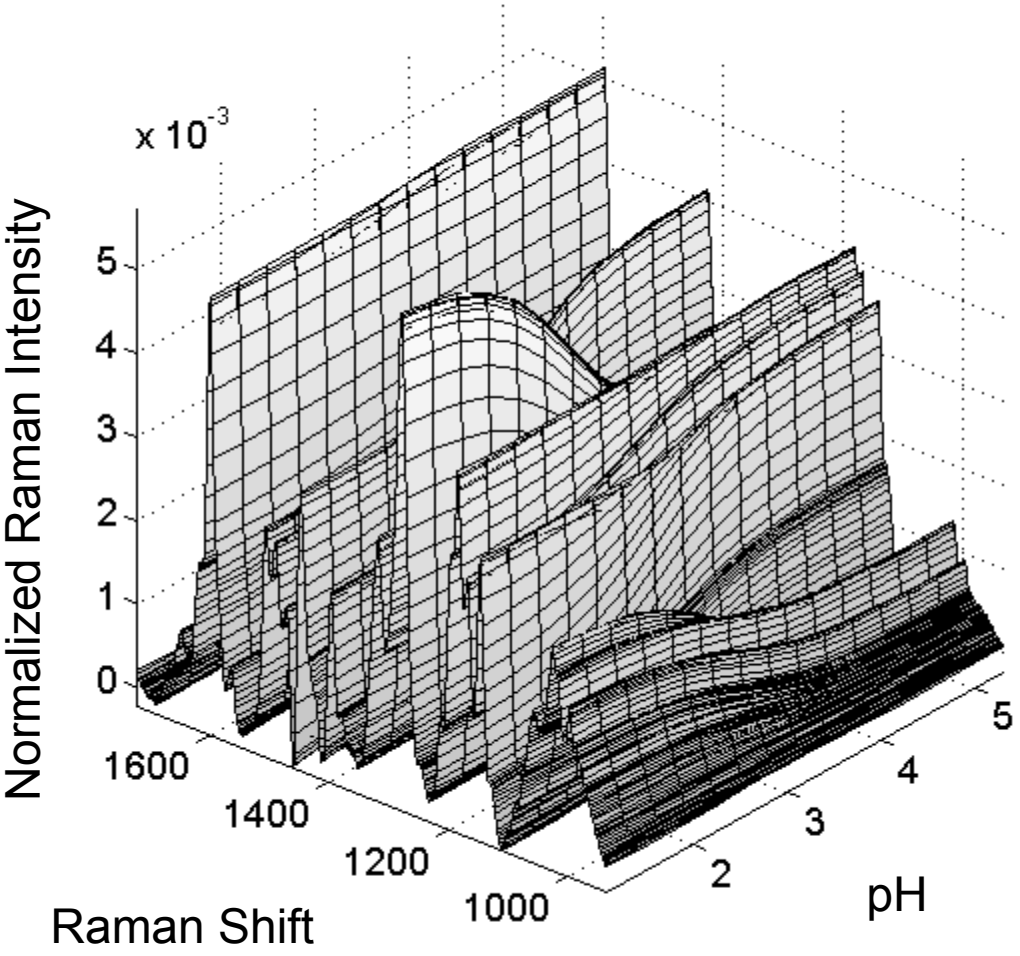
x 10^-3
Normalized Raman Intensity
5
4
3
2
1
0
1600
1400
1200
1000
Raman Shift
2
3
4
5
pH

Figure 7

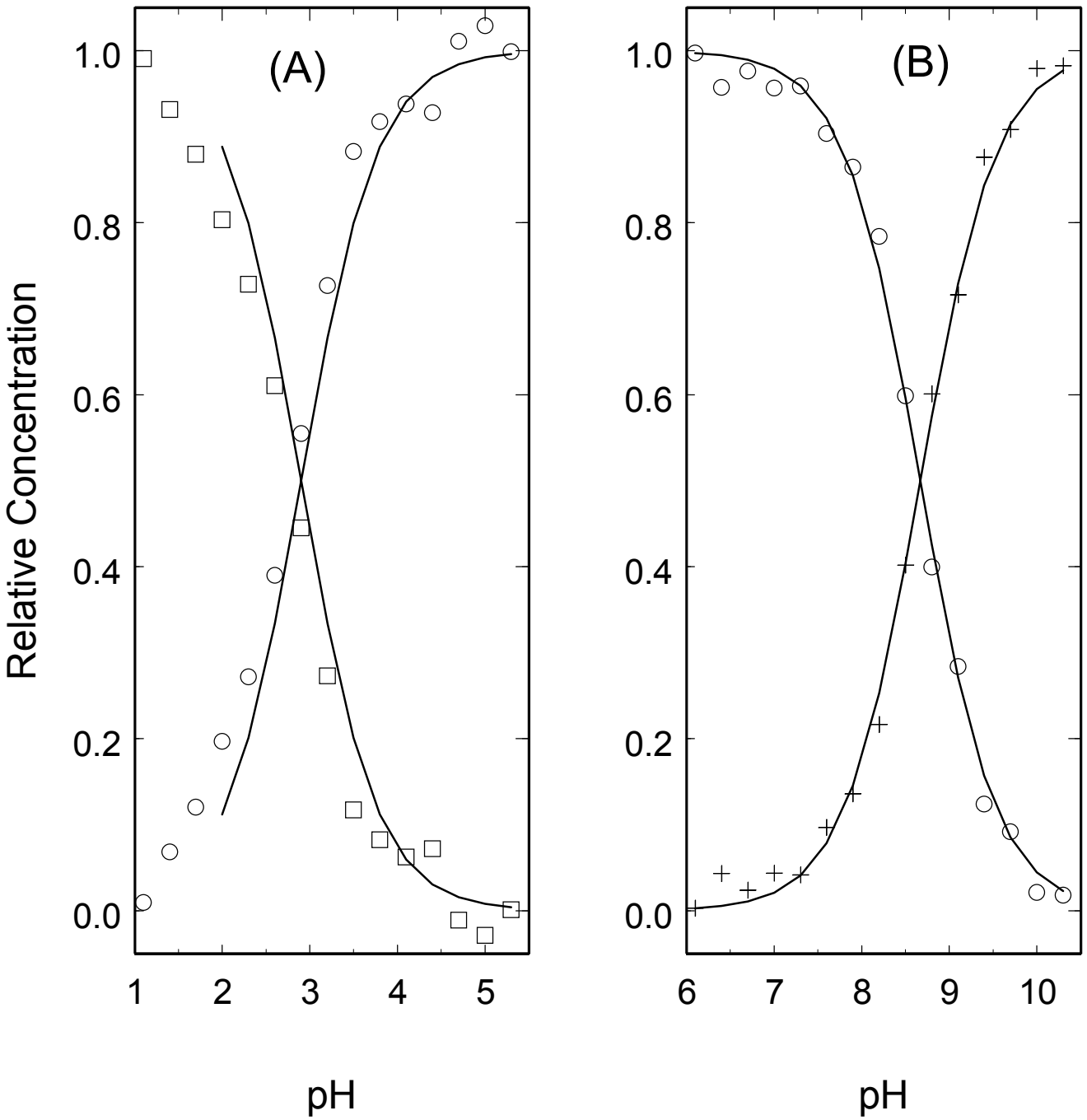
(A)
(B)
Relative Concentration
1.0
0.8
0.6
0.4
0.2
0.0
1
2
3
4
5
6
7
8
9
10
pH
pH

Figure 8

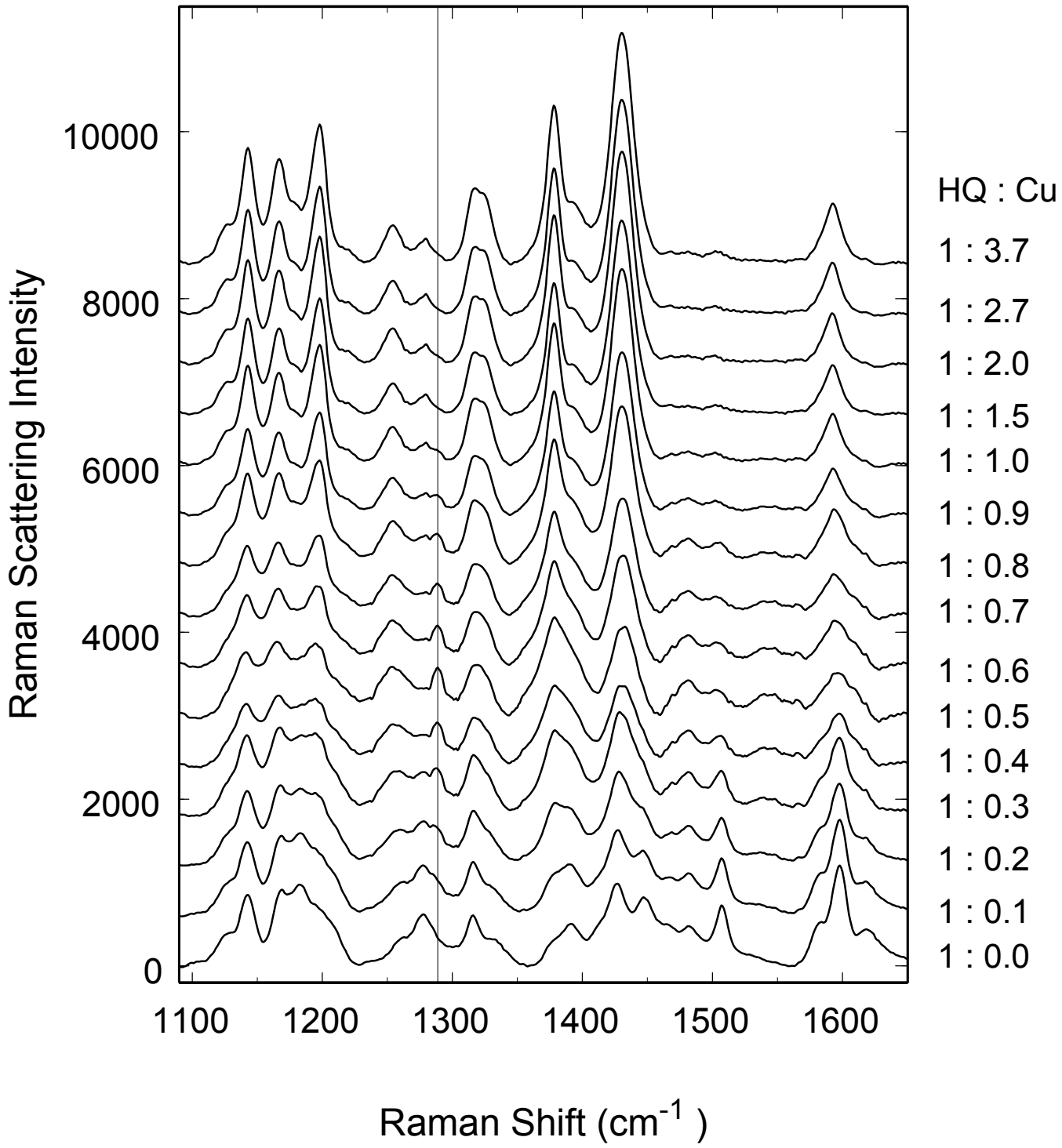
Raman Scattering Intensity
10000
8000
6000
4000
2000
0
1100
1200
1300
1400
1500
1600
Raman Shift (cm-1)
HQ : Cu
1 : 3.7
1 : 2.7
1 : 2.0
1 : 1.5
1 : 1.0
1 : 0.9
1 : 0.8
1 : 0.7
1 : 0.6
1 : 0.5
1 : 0.4
1 : 0.3
1 : 0.2
1 : 0.1
1 : 0.0

Figure 9

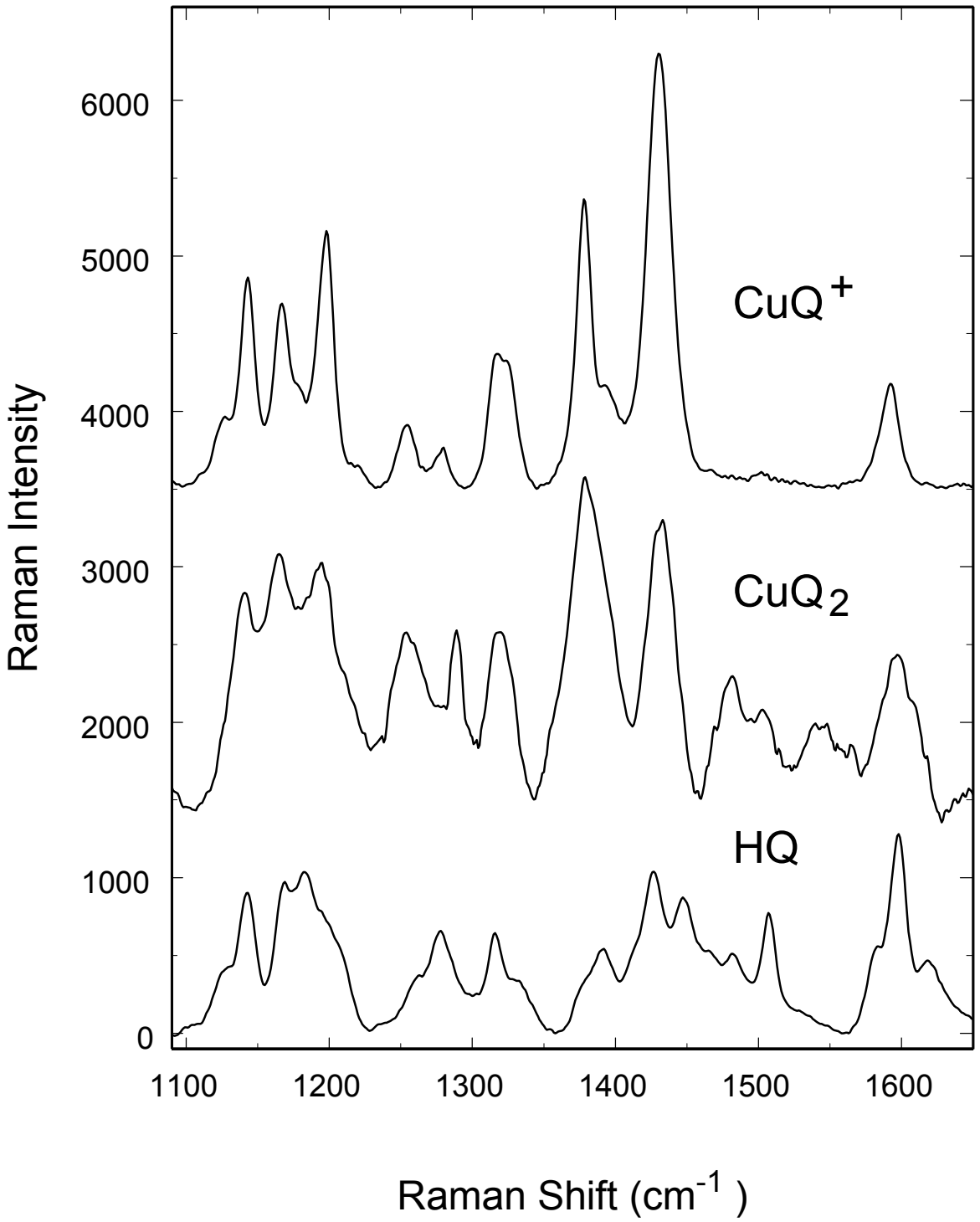
Raman Intensity
6000
5000
4000
3000
2000
1000
0
1100
1200
1300
1400
1500
1600
CuQ+
CuQ2
HQ
Raman Shift (cm-1)

Figure 10

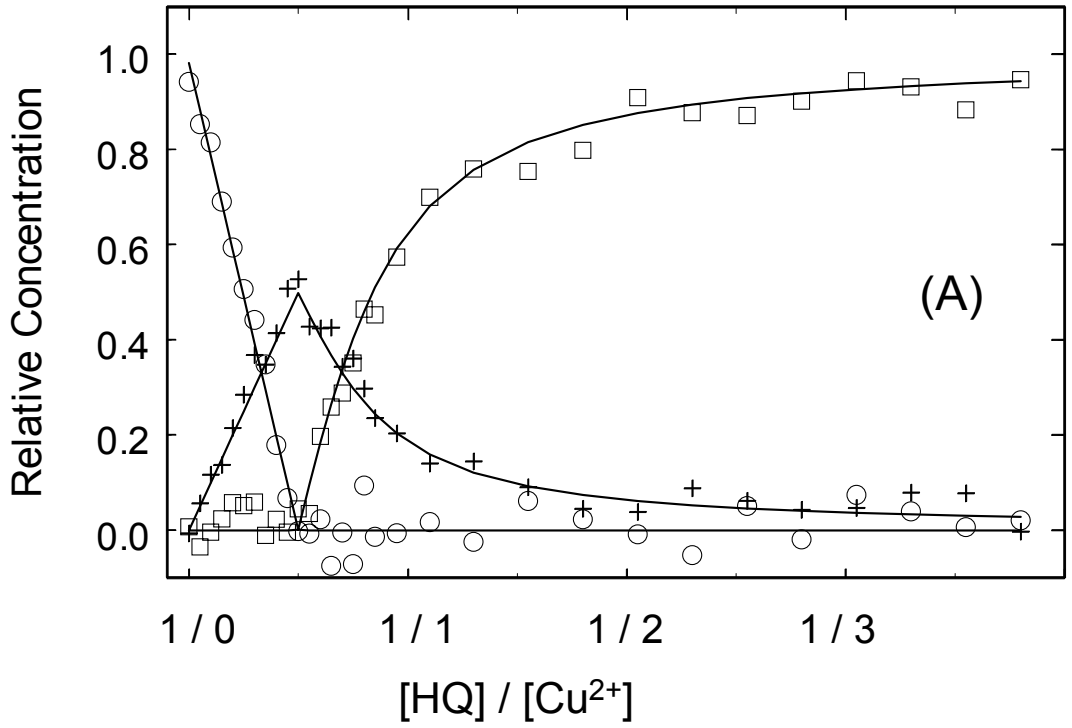
Relative Concentration
1.0
0.8
0.6
0.4
0.2
0.0
(A)
1 / 0
1 / 1
1 / 2
1 / 3
[HQ] / [Cu2+]

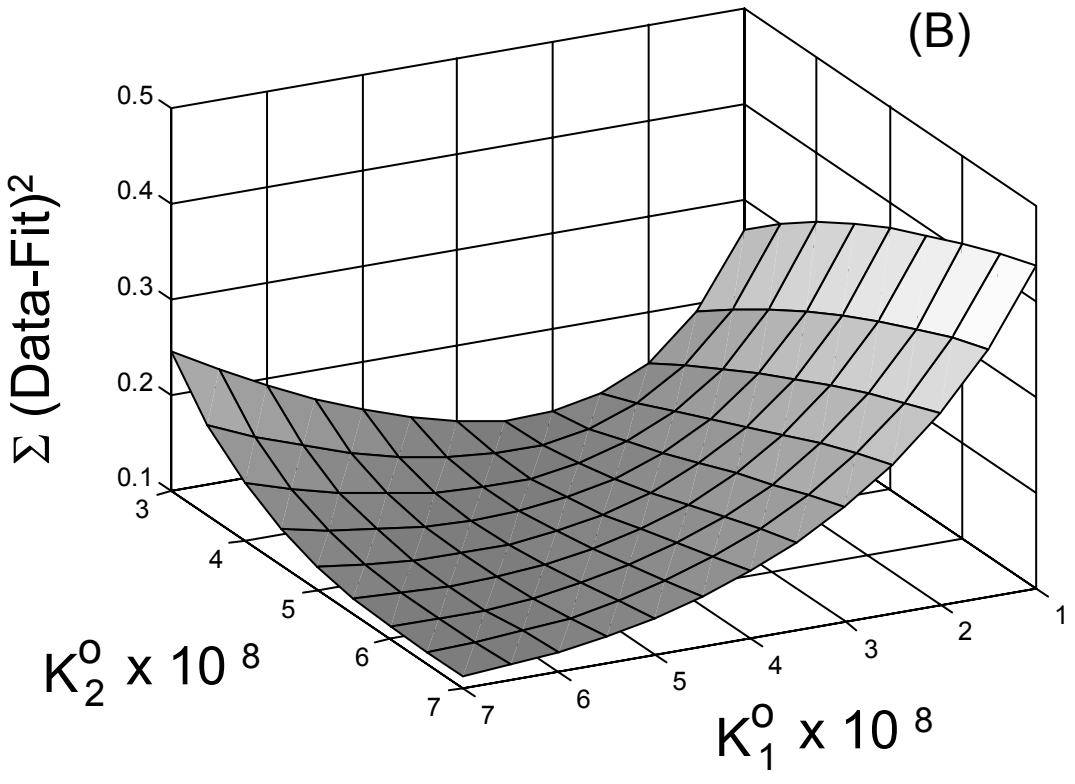
(B)
Σ (Data-Fit)2
0.5
0.4
0.3
0.2
0.1
3
4
5
6
7
K2o x 10 8
7
6
5
4
3
2
1
K1o x 10 8

Figure 11

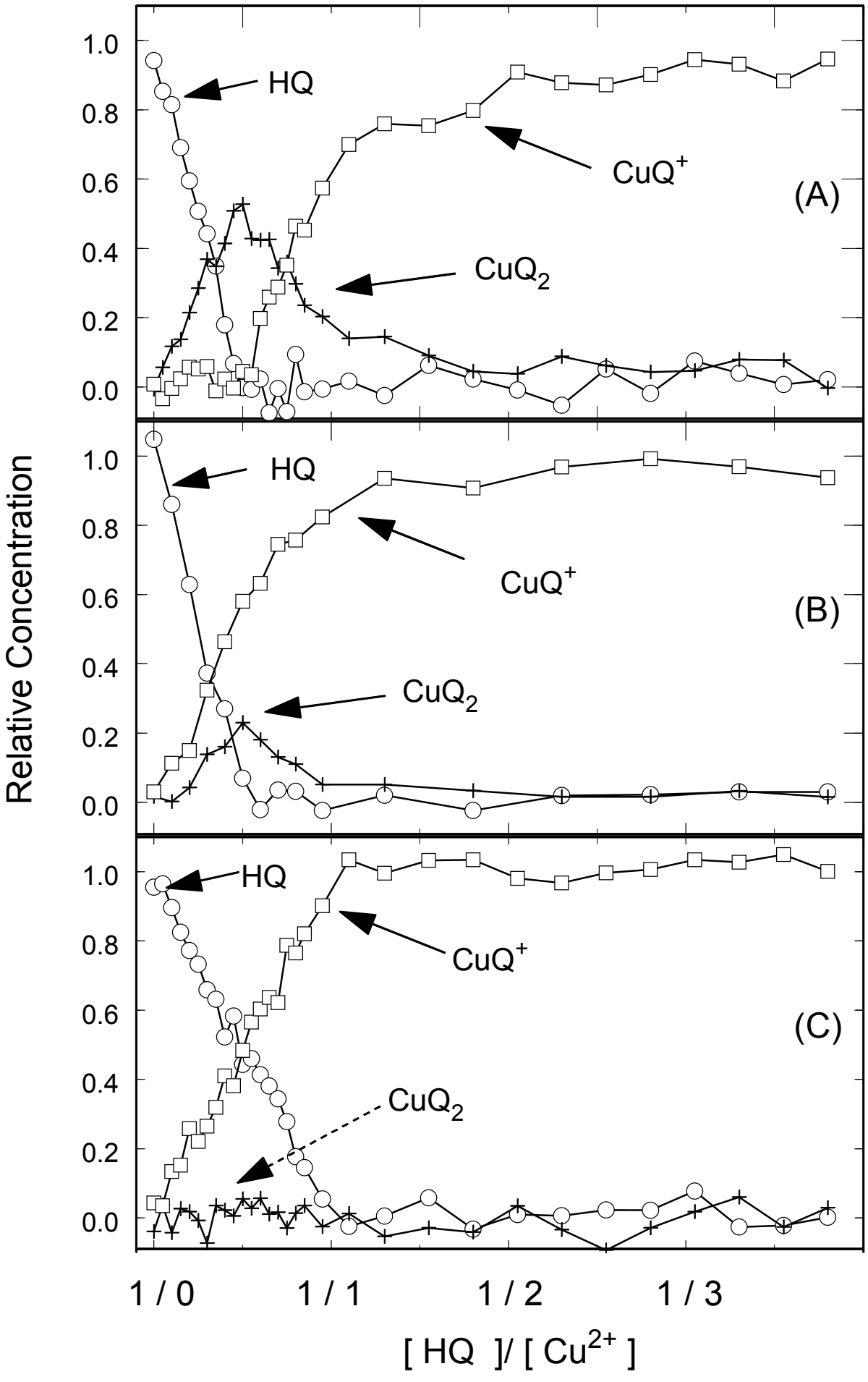
Relative Concentration
1.0
0.8
0.6
0.4
0.2
0.0
HQ
CuQ+
CuQ2
(A)
(B)
(C)
1 / 0
1 / 1
1 / 2
1 / 3
[HQ]/ [Cu2+]